

Cite this: *Chem. Sci.*, 2023, 14, 9024

All publication charges for this article have been paid for by the Royal Society of Chemistry

# Highly enantioselective synthesis of both tetrahydroquinoxalines and dihydroquinoxalinones via Rh–thiourea catalyzed asymmetric hydrogenation†

Ana Xu,<sup>a</sup> Chaoyi Li,<sup>a</sup> Junrong Huang,<sup>a</sup> Heng Pang,<sup>a</sup> Chengyao Zhao,<sup>a</sup> Lijuan Song,<sup>\*a</sup> Hengzhi You,<sup>ID \*ab</sup> Xumu Zhang,<sup>ID c</sup> and Fen-Er Chen,<sup>ID \*abd</sup>

Chiral tetrahydroquinoxalines and dihydroquinoxalinones represent the core structure of many bioactive molecules. Herein, a simple and efficient Rh–thiourea-catalyzed asymmetric hydrogenation for enantiopure tetrahydroquinoxalines and dihydroquinoxalinones was developed under 1 MPa H<sub>2</sub> pressure at room temperature. The reaction was magnified to the gram scale furnishing the desired products with undamaged yield and enantioselectivity. Application of this methodology was also conducted successfully under continuous flow conditions. In addition, <sup>1</sup>H NMR experiments revealed that the introduction of a strong Brønsted acid, HCl, not only activated the substrate but also established anion binding between the substrate and the ligand. More importantly, the chloride ion facilitated heterolytic cleavage of dihydrogen to regenerate the active dihydride species and HCl, which was computed to be the rate-determining step. Further deuterium labeling experiments and density functional theory (DFT) calculations demonstrated that this reaction underwent a plausible outer-sphere mechanism in this new catalytic transformation.

Received 13th February 2023

Accepted 3rd July 2023

DOI: 10.1039/d3sc00803g

rsc.li/chemical-science

## Introduction

Chiral 1,2,3,4-tetrahydroquinoxaline (THQ) and 3,4-dihydroquinoxalinone (DHQ) ring units are crucial motifs of many bioactive molecules.<sup>1</sup> Numerous optically pure THQs or DHQs have been developed as various pharmaceuticals or inhibitors. As shown in Fig. 1, the THQ fragment is an indispensable structural unit for cholesterol ester transfer protein (CETP) inhibitors in the treatment of atherosclerosis and obesity.<sup>2</sup> In addition, kinin B1 can treat inflammation and pain caused by septicemia, and GW420867X is a non-nucleoside HIV-1 reverse transcriptase inhibitor, which both embed the chiral DHQs as crucial motifs.<sup>3</sup> Therefore, developing efficient and concise methods to synthesize these compounds has attracted the attention of many chemistry researchers.<sup>4</sup> Pioneering catalytic

synthesis methods were established including intermolecular or intramolecular reaction with chiral substrates,<sup>5,6</sup> asymmetric transfer hydrogenation<sup>7</sup> and asymmetric hydrogenation.<sup>8</sup> Among these, using chiral substrates to prepare enantiopure THQs or DHQs usually required multiple reaction steps and the introduction of the corresponding optically pure amino alcohols or amino acids in advance.<sup>9</sup> On the other hand, asymmetric transfer hydrogenation which could simplify the reaction process, normally generated stoichiometric amounts of waste

<sup>a</sup>School of Science, Harbin Institute of Technology (Shenzhen), Taoyuan Street, Nanshan District, Shenzhen, 518055, China. E-mail: songlijuan@hit.edu.cn; youhengzhi@hit.edu.cn; rfchen@fudan.edu.cn

<sup>b</sup>Green Pharmaceutical Engineering Research Center, Harbin Institute of Technology (Shenzhen), Taoyuan Street, Nanshan District, Shenzhen, 518055, China

<sup>c</sup>Department of Chemistry, Shenzhen Grubbs Institute, Southern University of Science and Technology, Shenzhen 518055, China

<sup>d</sup>Engineering Center of Catalysis and Synthesis for Chiral Molecules, Department of Chemistry, Fudan University, Shanghai, 200433, China

† Electronic supplementary information (ESI) available. See DOI: <https://doi.org/10.1039/d3sc00803g>

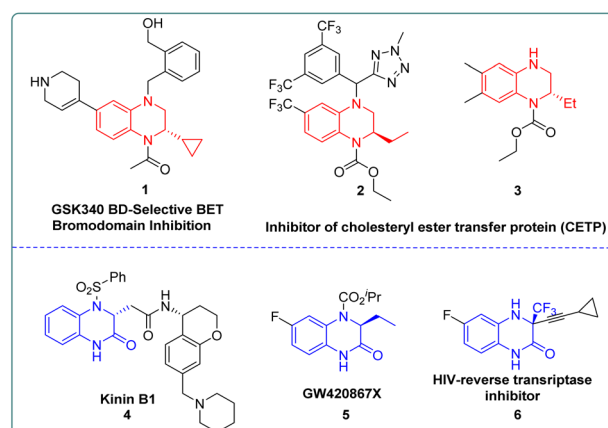
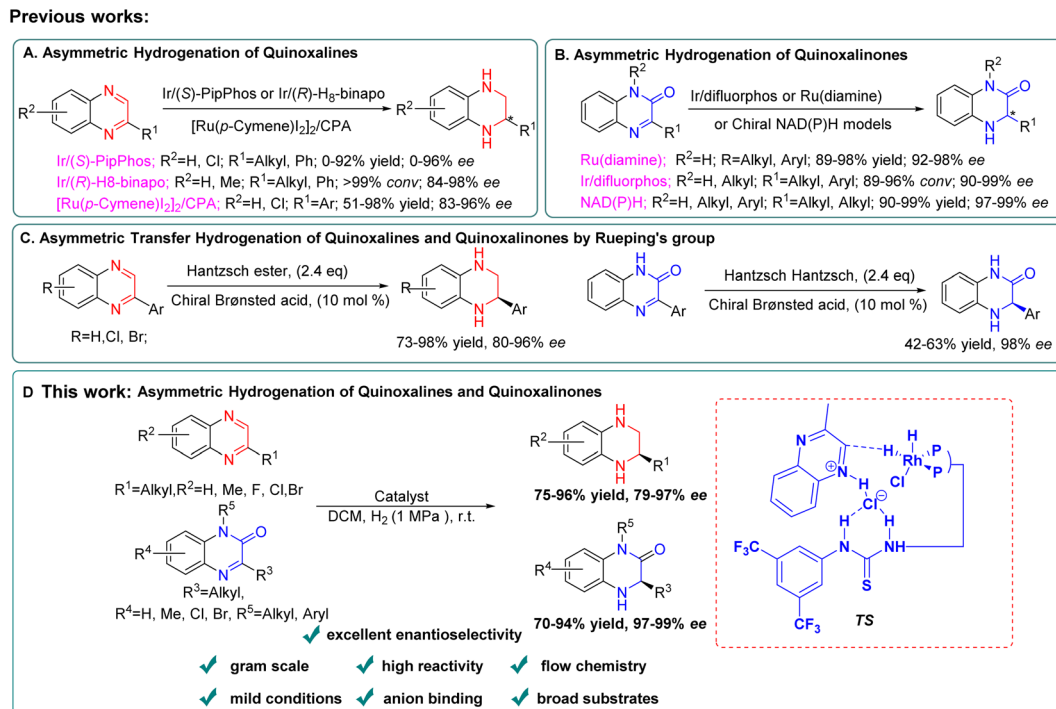


Fig. 1 Bioactive molecules with chiral THQs and DHQs.





Scheme 1 Asymmetric synthesis of chiral THQs and DHQs.

with the hydride source, leading to the reduction of the overall efficiency.<sup>7a,10</sup> By contrast, asymmetric hydrogenation exhibited many advantages such as atom economy, selectivity, functional group tolerance and product expandability, which received wide attention.<sup>11</sup>

For quinoxaline derivatives, Murata's group reported pioneering work on asymmetric hydrogenation using Rh-Diop in 1987, even though the desired product was only isolated in 3% ee.<sup>12</sup> Subsequently, other noble metals, such as Ir or Ru were explored with different bidentate ligands for asymmetric hydrogenation of quinoxaline derivatives with improved enantioselectivity (up to 90–90% ee).<sup>13</sup> Until 2009, the more general and efficient catalytic systems were developed employing monodentate phosphoramidite ligand (*S*)-PipPhos, (*R*)-H<sub>8</sub>-binapo and chiral phosphoric acid (CPA) separately (Scheme 1A).<sup>14</sup> For quinoxalinone derivatives, milestone studies were reported by Vidal-Ferran (Ir(P-OP)),<sup>8c</sup> Zhou (chiral NAD(P)H models)<sup>8d</sup> and Fan (Ru-diamine),<sup>3b</sup> respectively (Scheme 1B).

However, in these cases, limitations such as the use of toxic solvents,<sup>14c</sup> and the required high pressure<sup>3b</sup> and low temperature<sup>14b</sup> still existed making their broad industrial applications remain a challenge. In addition, these catalytic systems couldn't be simultaneously suitable for both asymmetric hydrogenation of quinoxalines and quinoxalinones. In 2010, Rueping's group reported the first general and efficient asymmetric transfer hydrogenation for quinoxalines and quinoxalinones using a Hantzsch ester and chiral Brønsted acid system, and the desired products were obtained with good to excellent enantioselectivities (Scheme 1C).<sup>7a</sup> But their substrate scope is still limited to aromatic substituents and it's not suitable for

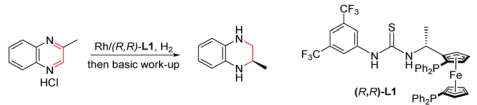
industrial applications due to the use of stoichiometric amounts of Hantzsch ester.

Very recently, Zhang's group successfully developed a combination of Brønsted acid and thiourea-diphosphone-transition metal catalyst systems for asymmetric hydrogenation of imines,<sup>15</sup> benzoxazinones,<sup>16</sup> nitroalkenes,<sup>17</sup> and quinolones<sup>18</sup> to prepare enantiopure hydrogenated products with high chemical activity and excellent enantioselectivity. Enlightened by these results, we developed a highly enantioselective method to construct both optically pure THQs and DHQs under the same catalytic conditions (Scheme 1D). A series of various substrates were converted to the corresponding products with excellent yields (up to 98%) and enantioselectivities (up to 99% ee). Furthermore, application of this methodology was conducted successfully under continuous flow conditions. This flow transformation greatly reduced the hazard of hydrogen accumulation in batch with shorter reaction time and is more friendly to scale-up. We also demonstrated the asymmetric hydrogenation process by which quinoxaline and quinoxalinone derivatives underwent anion binding between the substrate and ligand *via* a <sup>1</sup>H NMR mechanism study. In addition, the deuterium labeling experiments and density functional theory (DFT) calculations were conducted to gain more insight into the outer-sphere process of this new transformation and the origin of product enantioselectivity.

## Results and discussion

At the outset, we chose 2-methylquinoxaline hydrochloride (**1a**) as the model substrate to examine the efficiency of the Rh-thiourea-catalyst in this new transformation (Table 1). To our



Table 1 Optimization of the reaction conditions for asymmetric hydrogenation of 2-methylquinoxaline hydrochloride **1a**<sup>a</sup>


Entry	Solvent	Temp. (°C)	Time (h)	H <sub>2</sub> (MPa)	Conv. (%)	ee (%)
1	DCM : <sup>i</sup> PrOH = 2 : 1	40	24	4	99	91
2 <sup>b</sup>	DCM : <sup>i</sup> PrOH = 2 : 1	40	24	4	99	85
3	DCM : CHCl <sub>3</sub> = 2 : 1	40	24	4	99	90
4	EtOH	40	24	4	99	65
5	<sup>i</sup> PrOH	40	24	4	99	65
6	1,4-Dioxane	40	24	4	99	90
7	CHCl <sub>3</sub>	40	24	4	99	93
8	DCM	40	24	4	99	94
9	DCM	25	24	4	99	94
10	DCM	25	24	3	99	93
11	DCM	25	24	2	99	94
12	DCM	25	24	1	99	94
13	DCM	25	18	1	99/90 <sup>c</sup>	94/90 <sup>c</sup>
14 <sup>d</sup>	DCM	25	18	1	99/99 <sup>e</sup>	94/91 <sup>e</sup>
15 <sup>f</sup>	DCM	25	18	1	48	63

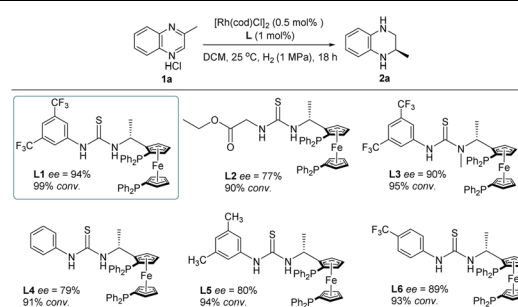
<sup>a</sup> Reaction conditions: **1a** (0.25 mmol) in 2 mL solvent, **1a**/[Rh(cod)Cl]<sub>2</sub>/ligand ratio = 100/0.5/1. <sup>b</sup> Catalytic precursor is [Ir(cod)Cl]<sub>2</sub>. <sup>c</sup> The reaction time is 12 h. <sup>d</sup> S/C = 1000. <sup>e</sup> S/C = 1500. <sup>f</sup> Without HCl. Conversion was determined by <sup>1</sup>H NMR analysis. ee was determined by HPLC.

delight, the corresponding hydrogenation product (**2a**) was isolated in 99% conversion with 91% ee under otherwise identical conditions to previously reported conditions (Table 1, entry 1).<sup>18a</sup> Encouraged by this initial result, we systematically investigated the influence of reaction parameters to enhance the reactivity and enantioselectivity. It was observed that the reaction could smoothly occur using [Ir(cod)Cl]<sub>2</sub> with a slight drop in enantioselectivity (Table 1, entry 2). Subsequently, we examined the effect of the solvents. When we replaced <sup>i</sup>PrOH with CHCl<sub>3</sub>, 99% conversion and 90% ee were obtained (Table 1, entry 3). In order to simplify the catalytic conditions, we performed the reaction in a single solvent. Polar protic solvents were found to give low enantioselectivities of products (Table 1, entries 4 and 5), while nonpolar aprotic solvents such as CHCl<sub>3</sub> and DCM could provide the target product with 93% and 94% ee separately (Table 1, entries 7 and 8). Finally, attempts to further improve the yield and/or enantioselectivity by tuning the reaction temperature, time, and pressure were also performed. The following optimum conditions were identified: [Rh(cod)Cl]<sub>2</sub> (0.5 mol%), (*R,R*)-**L1** (1 mol%) as a chiral ligand, and 18 h, in DCM and at 25 °C under a 1 MPa H<sub>2</sub> atmosphere. Notably, this good enantioselectivity could be realized at a molar substrate-to-catalyst (S/C) ratio of 1000, and the higher S/C ratio of 1500 showed a slightly lower enantioselectivity (Table 1, entry 14).

To explore the effects of diverse thiourea ligands on the control of the enantioselectivity of Rh-catalyzed quinoxaline asymmetric hydrogenation, we also synthesized a series of analogs of the **L1** ligand (Table 2). It was observed that the conversion rate and enantioselectivity of the reaction significantly dropped when using alkyl ester instead of aryl at the thiourea unit (**L2**). Furthermore, we found that the enantioselectivity of the reaction was sensitive to the substituents on the

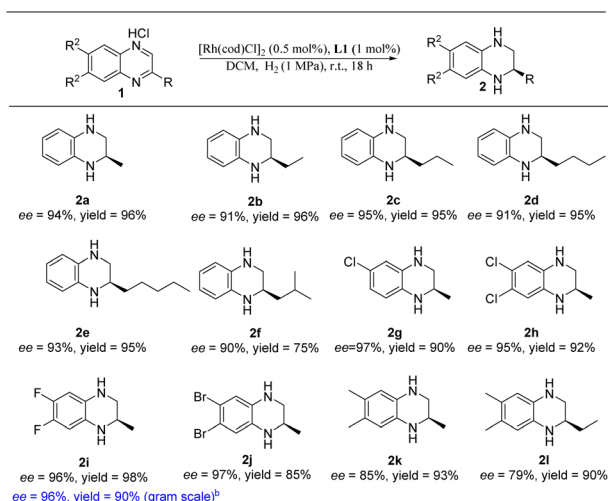
aryl ring (**L1**, **L4**, **L5** and **L6**). This observation was also reported by Hunger's group where the conformational dynamics and hydrogen-bonding dynamics of thiourea-based ligands caused by the difference in substitutions on the benzene ring play an important role in catalytic activities.<sup>19</sup> We also introduced an *N*-methyl on the thiourea unit (**L3**) which led to a slight decrease in catalytic activity. This phenomenon further confirmed the importance of secondary interaction between the chloride ion in the substrate and the hydrogen in the thiourea motif.

With the optimal reaction conditions in hand, we then evaluated the scope of quinoxaline derivatives (Table 3). Inspiringly, different alkyl substituents on C<sub>2</sub> of quinoxalines were completely hydrogenated to the desired products with high yields and enantioselectivities (**2a–2e**). Although the

Table 2 Ligand evaluation for asymmetric hydrogenation of 2-methylquinoxaline hydrochloride **1a**<sup>a</sup>

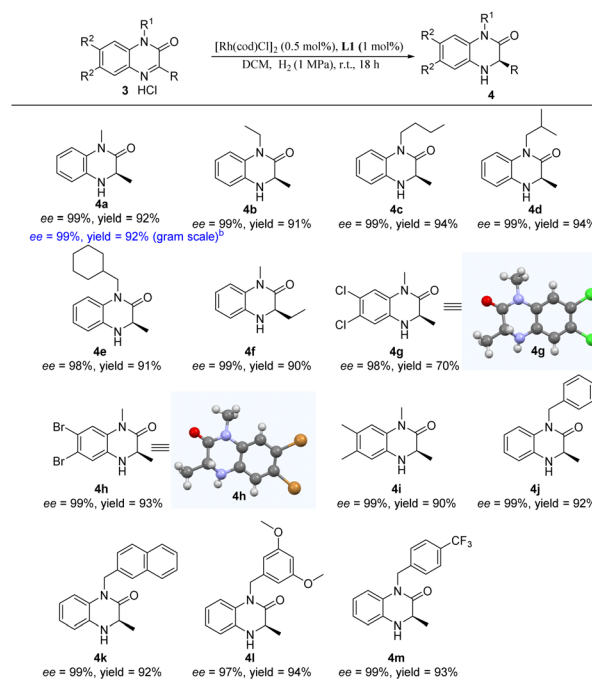
<sup>a</sup> Reaction conditions: **1a** (0.25 mmol) in 2 mL solvent, **1a**/[Rh(cod)Cl]<sub>2</sub>/ligand ratio = 100/0.5/1; conversion was determined by <sup>1</sup>H NMR analysis; ee was determined by HPLC.



Table 3 Scope of quinoxaline derivatives<sup>a</sup>

substrate bearing a 2-isobutyl substituent afforded the desired product with moderate yield, the enantioselectivity wasn't eroded (**2f**). It is worth noting that the dehalogenation of halogenated aromatic compounds which was often seen under transition-metal-catalyzed hydrogenation was not observed here.<sup>20</sup> Various halogenated groups such as Br, Cl and F were all tolerated under our hydrogenation system and delivered the desired products in excellent yields and enantioselectivities (**2g–2j**). In addition, the product enantioselectivity was found to be sensitive to the electron-donating groups on the aryl ring of the substrates (**2k–2l**). To further verify the practicability of this new Rh-thiourea-catalyzed quinoxaline asymmetric hydrogenation, we also magnified the reaction to the gram scale by using 6,7-difluoro-2-methyl-quinoxaline hydrochloride (**1i**) as the substrate. The reaction provided the corresponding product (**2i**) in 90% yield and 96% enantioselectivity without erosion.

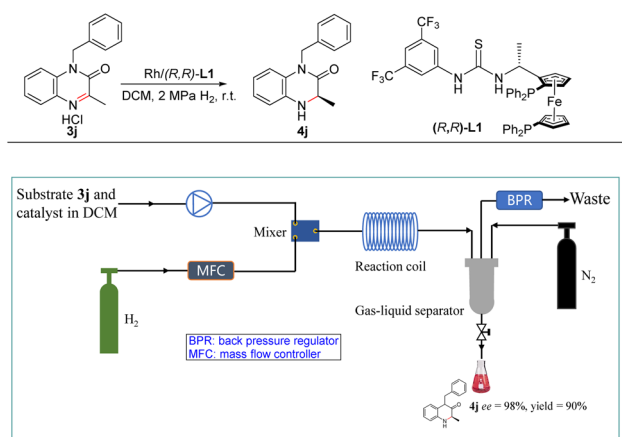
Encouraged by the excellent results of our catalytic system for asymmetric hydrogenation of quinoxaline derivatives, we envisioned that we could extend it to other heterocyclic substrates. The quinoxalinone substrate scope was evaluated as shown in Table 4. To our delight, substrates bearing various alkyl substituents at the N<sub>1</sub> position gave the corresponding products in excellent yields (91–94%) and enantioselectivities (98–99% ee) (**4a–4e**). In addition, we performed the gram-scale reaction of 1,3-dimethyl-2-quinoxalinone hydrochloride (**3a**) and afforded **4a** with undamaged yield and enantioselectivity. Furthermore, the substrate bearing an ethyl group at the C<sub>3</sub> position was smoothly reduced with high enantioselectivity (**4f**). Substrates with substituents at C<sub>6</sub> and C<sub>7</sub> positions of quinoxalinones also performed well to deliver the desired products in excellent yield with 98–99% ee (**4g–4i**). Moreover, the introduction of various arylmethyls at the N<sub>1</sub> position of substrates

Table 4 Scope of quinoxalinone derivatives<sup>a</sup>

afforded the corresponding hydrogenation products with excellent yield and enantioselectivity (**4j–4m**). Unfortunately, our catalytic system was found to be not tolerant for the substituents of <sup>t</sup>Pr, Cy, and the aromatic group (Table S1<sup>†</sup>). Among them, the configurations of **4g** and **4h** were assigned as *R* via single crystal X-ray diffraction (Tables S2 and S3<sup>†</sup>).

Recently, flow chemistry received remarkable attention in asymmetric hydrogenation because of advantages such as short residence time, high surface area-to-volume ratio, excellent reproducibility, easy scale-up, *etc.*<sup>21</sup> More importantly, this technology can reduce the hazards associated with the use of hydrogen gas which is highly flammable and forms an explosive mixture in air.<sup>22</sup> Therefore, this new Rh-catalysed asymmetric hydrogenation system was also applied to the continuous flow conditions (Scheme 2). First, solution of substrate **3j** and Rh-thiourea-catalyst was set in one stream, H<sub>2</sub> gas was set in another stream, and the two phases were sufficiently mixed through a microchip mixer. Then the relative parameters were investigated including the concentration of the substrate, gas velocity, liquid velocity, the pressure of H<sub>2</sub> and the residence time of this reaction (Table S5<sup>†</sup>). Finally, the desired product **4j** was obtained in high yield with excellent enantioselectivity at room temperature and 2 MPa H<sub>2</sub> within 25 min. Subsequently, a gram-scale continuous production was performed for this new Rh-catalysed asymmetric hydrogenation. 2.5 g product was obtained with 90% yield and 98% ee with more than 7.5 h with a high TON and TOF (180 and 428 h<sup>-1</sup>, respectively).





Scheme 2 Asymmetric homogeneous hydrogenation of substrate **3j** under continuous flow conditions.

In order to obtain insight into this new asymmetric hydrogenation mechanism, we first investigated the influence of hydrochloric acid. It was observed the model reaction using 2-methylquinoxaline as the substrate in the absence of hydrochloric acid gave 48% conversion with 63% ee in batch (Table 1 entry 15<sup>†</sup>). This result indicated that the strong Brønsted acid HCl was essential in this chemical transformation. Further observation reveals that the reaction rate is controlled by both Cl<sup>-</sup> and H<sup>+</sup>, and Cl<sup>-</sup> is also crucial for the ee value (Table S6<sup>†</sup>). We then mixed ligand **L1** with quinoxaline hydrochloride **1f** (3 eq.) and quinoxalinone hydrochloride **3a** (3 eq.) in CDCl<sub>3</sub>, respectively. The <sup>1</sup>H NMR study showed that the chemical shift of ligand **L1** shifted significantly downfield in both mixtures compared to single **L1** trace (Fig. 2). The original N–H peaks of thiourea were hidden in the aromatic peaks within 7.3–7.0 ppm, but they have shifted downfield to 10.92 ppm and 10.27 ppm in the mixture with **1f** (marked by a blue circle in Fig. 2). The N–H peak of thiourea moved to 10.62 ppm and 9.66 ppm in the mixture with **3a** (marked by a blue circle in Fig. 2). In addition,

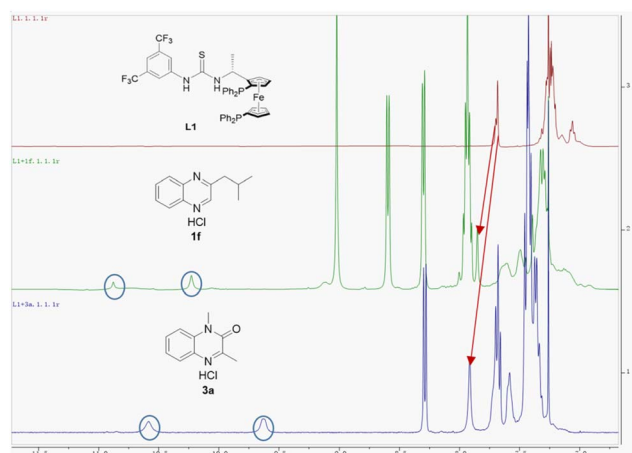


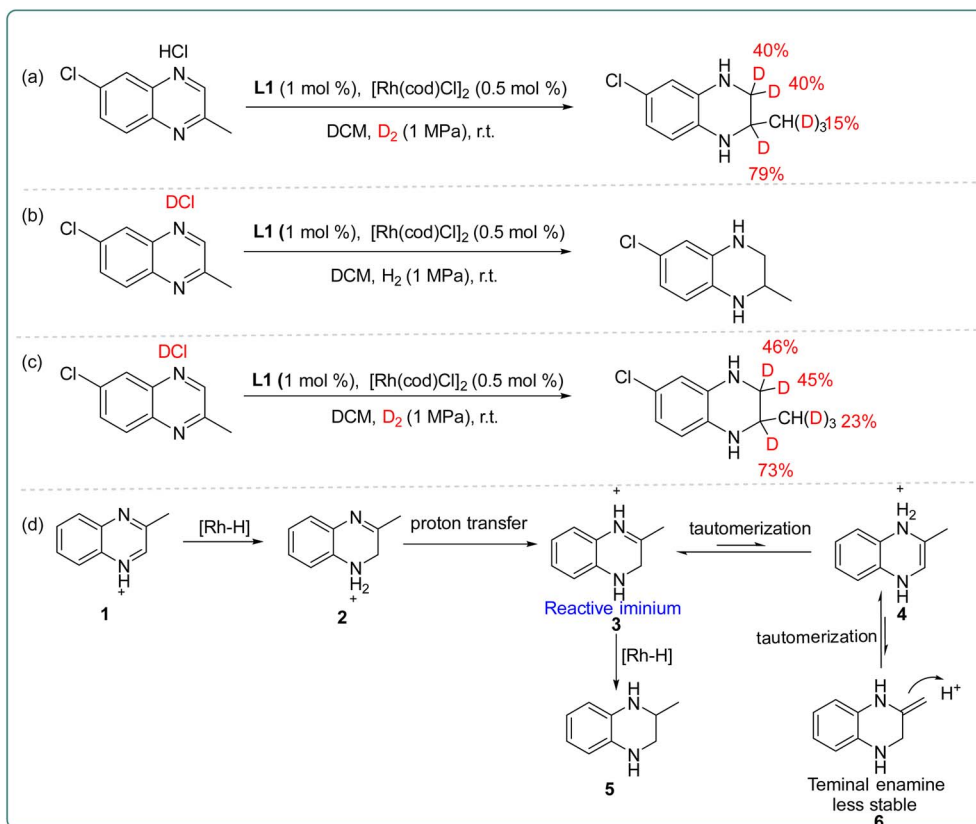
Fig. 2 <sup>1</sup>H NMR study of the interaction of **L1** (0.02 M) with **1f** (0.06 M) and **3a** (0.06 M) in CDCl<sub>3</sub>.

three hydrogen atoms on the 3,5-bis(trifluoromethyl)phenyl group of **L1** were also found to be shifted slightly downfield in both mixtures with **1f** and **3a** (marked by the red arrows in Fig. 2). In contrast, when quinoxaline is mixed directly with the ligand without preparing the salt in CDCl<sub>3</sub>, no recognition was observed (Fig. S4<sup>†</sup>). These results were consistent with the literature report,<sup>18a</sup> which showed that the anion bond formed between the chloride ion in the substrate and the hydrogen in the thiourea motif.

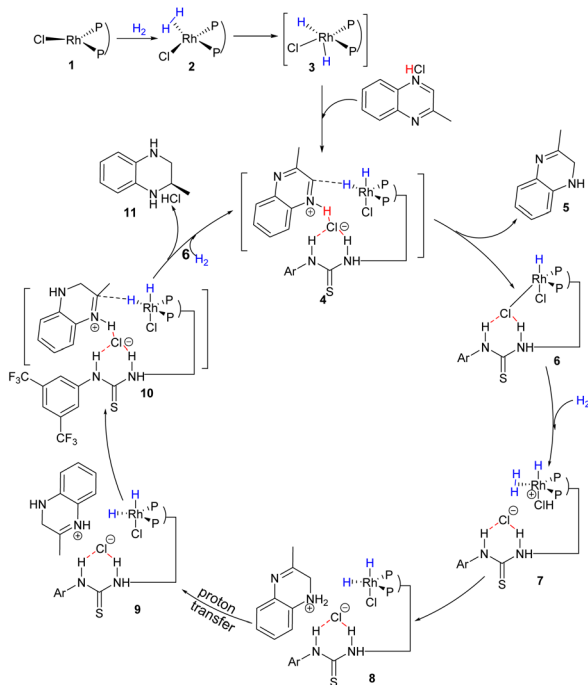
Subsequently, to further explore the source of hydrogen during the catalytic process, the deuterium labeling experiments were carried out as shown in Scheme 3. First, asymmetric hydrogenation of 6-chloro-2-methylquinoxaline hydrochloride was performed in D<sub>2</sub> gas, and the D atom was added at 2- and 3-positions (Scheme 3a). The experiment revealed that a small amount of deuteration occurred both in the normal hydrogen atom at the 3-position and the methyl group at the 2-position, which may be caused by tautomerism in the transformation process. Secondly, asymmetric hydrogenation was carried out in deuterated hydrochloride, and no deuterium product was observed (Scheme 3b). Finally, 6-chloro-2-methylquinoxaline deuterated hydrochloride was hydrogenated in D<sub>2</sub> (Scheme 3c), and the results were found to be similar to those in Scheme 3a. Based on these results, we proposed a possible transformation path (Scheme 3d). In the Rh–thiourea bisphosphine catalytic system, the oxidative addition of H<sub>2</sub> occurred; then the Rh–H bond broke, and the hydride was transferred to the C<sub>2</sub> position generating the partially reduced intermediate **2**. The intermediate **2** would not directly undergo the next hydrogenation, but went through proton transfer to generate the imine intermediate **3**, and then the enamine intermediates **4** and **6** were obtained through another tautomerism. In contrast, intermediate **3** was more stable and more prone to hydrogenation than intermediate **6**. Therefore, the hydrogenation happened from intermediate **3** to give the final product.

To further explore in more detail this new asymmetric hydrogenation mechanism, DFT calculations for asymmetric hydrogenation of 2-alkyl quinoxaline were also conducted. First, the linear effect experiment (Table S7 and Fig. S5<sup>†</sup>) and high-resolution mass spectroscopy (Fig. S6<sup>†</sup>) were conducted for investigation of the binding manner between the ligand and the chloride ion. This was different from Jacobsen's case which involved a 2 : 1 ratio.<sup>23</sup> The results suggested a 1 : 1 binding pattern. Here we proposed a plausible outer-sphere mechanism for this Rh-catalyzed quinoxaline asymmetric hydrogenation based on DFT calculations (Scheme 4 and Fig. 3).<sup>24</sup> First, 2-methylquinoxaline was protonated by HCl, and then, a catalyst–substrate complex **4** was formed. Simultaneously, the chloride ion formed hydrogen bonds with the thiourea of **L1** and the protonated 2-methylquinoxaline NH group. Then the hydride of the active rhodium complex was transferred to the substrate. Since previous protonation may happen on a different nitrogen, there were two possible carbon sites for hydrogen transfer (TS2-C<sub>1</sub> and TS2-C<sub>2</sub>, Fig. 3). The calculation results showed that the hydrogen transferred to the carbon with alkyl substitution *via* TS2-C<sub>2</sub> was 4.1 kcal mol<sup>-1</sup> higher in energy than the other. The first hydrogenation led to partially reductive intermediate **5**.





Scheme 3 Deuterium labeling experiment and the proposed transformation path.



Scheme 4 Outer-sphere mechanism for quinoxaline asymmetric hydrogenation.

Next, another  $H_2$  molecule coordinated with catalyst 6 formed intermediate 7, and the chloride ion facilitates heterolytic cleavage of dihydrogen to regenerate the active dihydride species and HCl, which was computed to be the rate-determining step. The transition states *via*  $TS3-N_1$  or  $TS3-N_4$  involved hydrogen transfer concerted with oxidative addition. Notably, the next protonation occurred at  $N_4$  directly as  $TS3-N_4$  showed  $6.2 \text{ kcal mol}^{-1}$  lower energy than  $TS3-N_1$ , which can be attributed to the  $sp^3$  nitrogen being more basic than the  $sp^2$  nitrogen. Therefore, the intermediate 8 was first produced and went through the process of proton transfer to generate a more stable intermediate 9. Then the active dihydride species will undergo a second recognition of the substrate *via* anion binding between the substrate and the ligand along with the insertion of hydride from a rhodium dihydride complex. The second hydride transferred preferentially to the Si-face at  $C_2$  of the protonated quinoxaline in the *R* configuration ( $TS4OR$ ) to generate product 11 and catalyst 6.  $TS4OR$  was computed to be lower in free energy than  $TS4OS$  by  $3.8 \text{ kcal mol}^{-1}$ , partly due to a larger distortion of the metal–ligand part in  $TS4OS$ , as indicated by the largely distorted dihedral angle of  $-47.97^\circ$  (Fig. S8<sup>†</sup>). In summary, our computational results were qualitatively consistent with the experimental observations and supported the cooperative effect of the Rh catalyst, Brønsted acid, and anion binding in asymmetric hydrogenation.



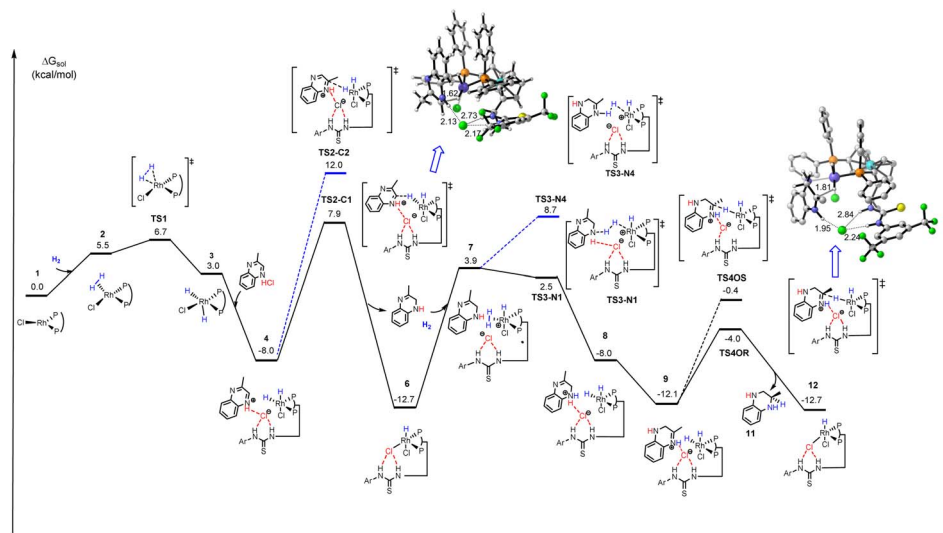


Fig. 3 DFT calculated energy potential surface for the proposed pathway (Ar = 3,5-di-CF<sub>3</sub>Ph; the phenyl groups on the phosphorus atoms are omitted for clarity; the relative Gibbs energies are labeled in kcal mol<sup>-1</sup>).

## Conclusions

In summary, a green, mild and practical asymmetric hydrogenation procedure to synthesize both enantiopure THQs and DHQs *via* a Rh-thiourea diphosphine catalytic system has been disclosed. The method allowed for the enantioselective transformation of various quinoxaline and quinoxalinone derivatives in excellent yields and enantioselectivities. In addition, the reactions were magnified to the gram scale under both batch and continuous flow conditions without erosion of the catalyst activity and enantiomeric excess. The <sup>1</sup>H NMR experiments show that the introduction of the strong Brønsted acid HCl played an important role both in activating the substrate and establishing anion binding between the substrate and the ligand in this new Rh-catalyzed asymmetric hydrogenation. Deuterium labeling experiments revealed that equilibrium tautomerism occurred between enamine and imine after the first hydrogenation. The later detailed DFT calculations further demonstrated an outer-sphere mechanism for this new transformation. We anticipate that this work will provide a milder and more practical synthetic tool for the efficient and highly enantioselective synthesis of both THQs and DHQs. The mechanistic studies, as well as the continuous flow application, will aid in enlightening further efficient and industrially friendly processes for asymmetric hydrogenation.

## Data availability

Our experimental or computational data associated with this article have been deposited in ESI.†

## Author contributions

The manuscript was written through contributions of all authors. All authors have given approval to the final version of the manuscript.

## Conflicts of interest

There are no conflicts to declare.

## Acknowledgements

This work was supported by Shenzhen Science and Technology Research Fund No. JCYJ20190806142203709; JSGG20191129114029286; JSGG20201103153807021; GXWD20220811173736002. We were also grateful to Guangdong Basic, Applied Basic Research Foundation (No. 2021A1515110366) and Shenzhen Key Laboratory of Advanced Functional Carbon Materials Research and Comprehensive Application. We appreciate the guidance and opinions from Professor Xu-Mu Zhang.

## Notes and references

- (a) S. Fleischer, S. L. Zhou, S. Werkmeister, K. Junge and M. Beller, Cooperative Iron-Brønsted Acid Catalysis: Enantioselective Hydrogenation of Quinoxalines and 2-H-1,4-Benzoxazines, *Chem. – Eur. J.*, 2013, **19**, 4997–5003; (b) W. J. Tang, J. Tan, L. J. Xu, K. H. Lam, Q. H. Fan and A. Chan, Highly Enantioselective Hydrogenation of Quinoline and Pyridine Derivatives with Iridium-(P-Phos) Catalyst, *Adv. Synth. Catal.*, 2010, **352**, 1055–1062; (c) Z. B. Zhao, X. Li, M. W. Chen, Z. K. Zhao and Y. G. Zhou, Biomimetic asymmetric reduction of benzoxazinones and quinoxalinones using ureas as transfer catalysts, *Chem. Commun.*, 2020, **56**, 7309–7312.
- (a) F. Shi, W. Tan, H. H. Zhang, M. Li, Q. Ye, G. H. Ma, S. J. Tu and G. G. Li, Asymmetric Organocatalytic Tandem Cyclization/Transfer Hydrogenation: A Synthetic Strategy for Enantioenriched Nitrogen Heterocycles, *Adv. Synth. Catal.*, 2013, **355**(18), 3715–3726; (b) S. Fleischer,



- S. L. Zhou, S. Werkmeister, K. Junge and M. Beller, Cooperative Iron-Brønsted Acid Catalysis: Enantioselective Hydrogenation of Quinoxalines and 2-H-1,4-Benzoxazines, *Chem. – Eur. J.*, 2013, **19**(16), 4997–5003; (c) Z. Yao, Z. I. Luo, Y. X. Pan, X. Zhang, B. H. Li, L. J. Xu, P. Wang and Q. Shi, Metal-Free Tandem One-Pot Construction of 3,3-Disubstituted 3,4-Dihydroquinoxalin-2(1H)-Ones under Visible-Light Photoredox Catalysis, *Adv. Synth. Catal.*, 2021, **364**(3), 658–664.
- 3 (a) Y. Y. Peng, M. W. Chen, Z. Deng, Q. Yang and J. Huang, Enantioselective synthesis of trifluoromethylated dihydroquinoxalinones via palladium-catalyzed hydrogenation, *Org. Chem. Front.*, 2019, **6**, 746–750; (b) C. H. Li, S. X. Zhang, S. Li, Y. Peng and Q. H. Fan, Ruthenium-catalyzed enantioselective hydrogenation of quinoxalinones and quinazolinones, *Org. Chem. Front.*, 2022, **9**(2), 400–406.
- 4 (a) D. Cartigny, F. Berhal, T. Nagano, P. Phansavath, T. Ayad, J. P. Genêt, T. Ohshima, K. Mashima and V. Ratovelomanana-Vidal, General Asymmetric Hydrogenation of 2-Alkyl- and 2-Aryl-Substituted Quinoxaline Derivatives Catalyzed by Iridium-Difluorophos: Unusual Halide Effect and Synthetic Application, *Chem. – Eur. J.*, 2012, **77**(10), 4544–4556; (b) T. Nagano, A. Iimuro, R. Schwenk, T. Ohshima, Y. Kita, A. Togni and K. Mashima, Additive Effects of Amines on Asymmetric Hydrogenation of Quinoxalines Catalyzed by Chiral Iridium Complexes, *Chem. – Eur. J.*, 2012, **18**(37), 11578–11592.
- 5 M. Imanishi, M. Sonoda, H. Miyazato, K. Sugimoto, M. Akagawa and S. Tanimori, Sequential Synthesis, Olfactory Properties, and Biological Activity of Quinoxaline Derivatives, *ACS Omega*, 2017, **2**(5), 1875–1885.
- 6 K. Samanta, N. Srivastava, S. Saha and G. Panda, Inter- and intramolecular Mitsunobu reaction and metal complexation study: synthesis of  $\alpha$ -amino acids derived chiral 1,2,3,4-tetrahydroquinoxaline, benzo-annulated [9]-N3 peraza, [12]-N4 peraza-macrocycles, *Org. Biomol. Chem.*, 2012, **10**(8), 1553–1564.
- 7 (a) M. Rueping, F. Tato and F. R. Schoepke, The First General, Efficient and Highly Enantioselective Reduction of Quinoxalines and Quinoxalinones, *Chem. – Eur. J.*, 2010, **16**, 2688–2691; (b) T. Jing, W. Tang, Y. Sun, J. Zhen and J. Xiao, pH-Regulated transfer hydrogenation of quinoxalines with a Cp\*Ir-diamine catalyst in aqueous media, *Cheminform*, 2011, **67**(34), 6206–6213; (c) Z. Y. Xue, Y. Jiang, X. Z. Peng, W. C. Yuan and X. M. Zhang, The First General, Highly Enantioselective Lewis Base Organocatalyzed Hydrosilylation of Benzoxazinones and Quinoxalinones, *Adv. Synth. Catal.*, 2010, **352**(13), 2132–2136.
- 8 (a) J. Qin, F. Chen, Z. Y. Ding, Y. M. He, L. J. Xu and Q. H. Fan, Asymmetric Hydrogenation of 2- and 2,3-Substituted Quinoxalines with Chiral Cationic Ruthenium Diamine Catalysts, *Org. Lett.*, 2011, **13**(24), 6569–6571; (b) S. Sun and P. Nagorny, Exploration of chiral diastereomeric spiroketal (SPIROL)-based phosphinite ligands in asymmetric hydrogenation of heterocycles, *Chem. Commun.*, 2020, **56**(60), 8432–8435; (c) Z. Zhang and H. F. Du, A Highly cis-Selective and Enantioselective Metal-Free Hydrogenation of 2,3-Disubstituted Quinoxalines, *Angew. Chem., Int. Ed.*, 2015, **54**, 623–626; (d) Z. H. Zhu, Y. X. Ding and Y. G. Zhou, Biomimetic reduction of imines and heteroaromatics with chiral and regenerable [2.2] Paracyclophane-Based NAD(P)H model CYNAM, *Tetrahedron*, 2021, **83**, 131968; (e) J. Rico and A. Vidal-Ferran, [Ir(P-OP)]-Catalyzed Asymmetric Hydrogenation of Diversely Substituted C=N Containing Heterocycles, *Org. Lett.*, 2013, **15**, 2066–2069.
- 9 (a) J. F. Bower, P. Szeto and T. Gallagher, Enantiopure 1,4-Benzoxazines via 1,2-Cyclic Sulfamidates. Synthesis of Levofloxacin, *Org. Lett.*, 2007, **9**, 3283–3286; (b) N. Selvakumar, B. Yadi Reddy, G. Sunil Kumar, M. K. Khera, D. Srinivas, M. Sitaram Kumar, J. Das, J. Iqbal and S. Trehan, Synthesis of novel tricyclic oxazolidinones by a tandem SN2 and SNAr reaction: SAR studies on conformationally constrained analogues of Linezolid, *Bioorg. Med. Chem. Lett.*, 2006, **16**(16), 4416–4419.
- 10 X. F. Cai, R. N. Guo, G. S. Feng, B. Wu and Y. G. Zhou, Chiral phosphoric acid-catalyzed asymmetric transfer hydrogenation of quinolin-3-amines, *Org. Lett.*, 2014, **16**, 2680–2683.
- 11 (a) Y. Hu, Z. Zhang, J. Zhang, Y. Liu and W. Zhang, Cobalt-Catalyzed Asymmetric Hydrogenation of C=N Bonds Enabled by Assisted Coordination and Nonbonding Interactions, *Angew. Chem., Int. Ed.*, 2019, **58**, 15767–15771; (b) F. H. Zhang, F. J. Zhang, M. L. Li, J. H. Xie and Q. L. Zhou, Enantioselective hydrogenation of dialkyl ketones, *Nat. Catal.*, 2020, **3**(8), 621–627; (c) Y. Hu, Z. Zhang, Y. Liu and W. Zhang, Cobalt-Catalyzed Chemo- and Enantioselective Hydrogenation of Conjugated Enynes, *Angew. Chem., Int. Ed.*, 2021, **60**, 16989–16993; (d) C. G. Liu, M. Y. Wang, Y. H. Xu, Y. B. Li and Q. Liu, Manganese-Catalyzed Asymmetric Hydrogenation of 3H-Indoles, *Angew. Chem., Int. Ed.*, 2022, **61**(20), e202202814; (e) C. G. Liu, M. Y. Wang, S. H. Liu, Y. J. Wang, Y. Peng, Y. Lan and Q. Liu, Manganese-Catalyzed Asymmetric Hydrogenation of Quinolines Enabled by  $\pi$ - $\pi$  Interaction, *Angew. Chem., Int. Ed.*, 2021, **60**(10), 5108–5113; (f) Z. Wei, F. Shao and J. Wang, Recent advances in heterogeneous catalytic hydrogenation and dehydrogenation of N-heterocycles, *Chin. J. Catal.*, 2019, **40**(7), 980–1002; (g) R. Gunasekar, R. L. Goodyear, I. P. Silvestri and J. Xiao, Recent developments in enantio- and diastereoselective hydrogenation of N-heteroaromatic compounds, *Org. Biomol. Chem.*, 2022, **20**(9), 1794–1827.
- 12 S. Murata, T. Sugimoto and S. Matsuura, Hydrogenation and hydrosilylation of quinoxaline by homogeneous rhodium catalysts, *Heterocycles*, 1987, **26**(3), 763–766.
- 13 (a) J. P. Henschke, M. J. Burk, C. G. Malan, D. Herzberg, J. A. Peterson, A. J. Wildsmith, C. J. Cobley and G. Casy, Synthesis and Applications of HexaPHEMP, a Novel Biaryl Diphosphine Ligand, *Adv. Synth. Catal.*, 2003, **345**(12), 300–307; (b) L. Q. Qiu, F. Y. Kwong, J. Wu, W. H. Lam,





- S. S. Chan, W. Y. Yu, Y. M. Li, R. W. Guo, Z. Y. Zhou and A. S. C. Chan, A New Class of Versatile Chiral Bridged Atropisomeric Diphosphine Ligands: Remarkably Efficient Ligand Syntheses and Their Applications in Highly Enantioselective Hydrogenation Reactions, *J. Am. Chem. Soc.*, 2006, **128**, 5955–5965; (c) C. J. Cobley and J. P. Henschke, Enantioselective Hydrogenation of Imines Using a Diverse Library of Ruthenium Dichloride(diphosphine)(diamine) Precatalysts, *Adv. Synth. Catal.*, 2003, **345**(12), 195–201; (d) C. Bianchini, P. Barbaro, G. Scapacci, E. Farnetti and M. Graziani, Enantioselective Hydrogenation of 2-Methylquinoxaline to (-)-(2S)-2-Methyl-1,2,3,4-tetrahydroquinoxaline by Iridium Catalysis, *Organometallics*, 1998, (17), 3308–3310.
- 14 (a) N. Mršić, T. Jerphagnon, A. J. Minnaard, B. L. Feringa and J. G. de Vries, Asymmetric Hydrogenation of Quinoxalines Catalyzed by Iridium/PipPhos, *Adv. Synth. Catal.*, 2009, **351**(16), 2549–2552; (b) W. J. Tang, L. J. Xu, Q. H. Fan, J. Wang, B. M. Fan, Z. Y. Zhou, K. H. Lam and A. S. C. Chan, Asymmetric Hydrogenation of Quinoxalines with Diphosphinite Ligands: A Practical Synthesis of Enantioenriched, Substituted Tetrahydroquinoxalines, *Angew. Chem., Int. Ed.*, 2009, **48**, 9135–9138; (c) Q. A. Chen, D. S. Wang, Y. G. Zhou, D. Ying, H. J. Fan, Y. Yan and Z. Zhang, Convergent Asymmetric Disproportionation Reactions: Metal/Brønsted Acid Relay Catalysis for Enantioselective Reduction of Quinoxalines, *J. Am. Chem. Soc.*, 2011, **133**, 6126–6129.
- 15 (a) Q. Zhao, J. Wen, R. Tan, K. Huang, P. Metola, R. Wang, E. V. Anslyn and X. Zhang, Rhodium-catalyzed asymmetric hydrogenation of unprotected NH imines assisted by a thiourea, *Angew. Chem., Int. Ed.*, 2014, **53**(32), 8467–8470; (b) P. Li, Y. Huang, X. Q. Hu, X. Q. Dong and X. M. Zhang, Access to Chiral Seven-Member Cyclic Amines via Rh-Catalyzed Asymmetric Hydrogenation, *Org. Lett.*, 2017, **19**(14), 3855–3858.
- 16 Z. Han, G. Liu, R. Wang, X. Q. Dong and X. Zhang, Highly efficient Ir-catalyzed asymmetric hydrogenation of benzoxazinones and derivatives with a Brønsted acid cocatalyst, *Chem. Sci.*, 2019, **10**(15), 4328–4333.
- 17 Q. Y. Zhao, S. K. Li, K. X. Huang, R. Wang and X. M. Zhang, A Novel Chiral Bisphosphine-Thiourea Ligand for Asymmetric Hydrogenation of  $\beta,\beta$ -Disubstituted Nitroalkenes, *Org. Lett.*, 2013, **15**(15), 4014–4017.
- 18 (a) J. Wen, R. Tan, S. Liu, Q. Zhao and X. Zhang, Strong Brønsted acid promoted asymmetric hydrogenation of isoquinolines and quinolines catalyzed by a Rh-thiourea chiral phosphine complex via anion binding, *Chem. Sci.*, 2016, **7**, 3047–3051; (b) Z. Y. Han, G. Liu, X. L. Yang, X. Q. Dong and X. M. Zhang, Enantiodivergent Synthesis of Chiral Tetrahydroquinoline Derivatives via Ir-Catalyzed Asymmetric Hydrogenation: Solvent-Dependent Enantioselective Control and Mechanistic Investigations, *ACS Catal.*, 2021, **11**, 7281–7291.
- 19 A. A. Ehrhard, L. Gunkel, S. Jager, A. C. Sell, Y. Nagata and J. Hunger, Elucidating Conformation and Hydrogen-Bonding Motifs of Reactive Thiourea Intermediates, *ACS Catal.*, 2022, **12**(20), 12689–12700.
- 20 (a) K. Omari-Qadry, K. Hamza, Y. Sasson and J. Blum, Liquid phase hydrodechlorination of some chlorinated aromatic nitrogen-containing heterocyclics, *J. Mol. Catal. A: Chem.*, 2009, **308**, 182–185; (b) M. Martin-Martinez and L. M. Gómez-Sainero, Progress in Catalytic Hydrodechlorination, *Catalysts*, 2021, **11**, 1–2; (c) L. M. Gómez-Sainero, J. Palomar, S. Omar, C. Fernández, J. Bedia, A. Álvarez-Montero and J. J. Rodríguez, Valorization of chloromethanes by hydrodechlorination with metallic catalysts, *Catal. Today*, 2018, **310**, 75–85.
- 21 (a) P. J. Cossar, L. Hizartidis, M. I. Simone, A. McCluskey and C. P. Gordon, The expanding utility of continuous flow hydrogenation, *Org. Biomol. Chem.*, 2015, **13**(26), 7119–7130; (b) J. Y. Liao, S. L. Zhang, Z. S. Wang, X. Song, D. L. Zhang, R. Kumar, J. Jin, P. Ren, H. Z. You and F. E. Chen, Transition-metal catalyzed asymmetric reactions under continuous flow from 2015 to early 2020, *Green Synth. Catal.*, 2020, **1**(2), 121–133; (c) F. Guan, A. J. Blacker, B. Hall, N. Kapur, J. Wen and X. Zhang, High-pressure asymmetric hydrogenation in a customized flow reactor and its application in multi-step flow synthesis of chiral drugs, *J. Flow Chem.*, 2021, **11**(4), 763–772; (d) W. Li, M. Jiang, M. Liu, X. Ling, Y. Xia, L. Wan and F. Chen, Development of a Fully Continuous-Flow Approach Towards Asymmetric Total Synthesis of Tetrahydroprotoberberine Natural Alkaloids, *Chemistry*, 2022, **28**(33), e202200700; (e) J. Wang, J. Li, Y. Wang, S. He, H. You and F.-E. Chen, Polymer-Supported Chiral Heterogeneous Copper Catalyst for Asymmetric Conjugate Addition of Ketones and Imines under Batch and Flow, *ACS Catal.*, 2022, **12**(15), 9629–9637.
- 22 R. Porcar, A. Mollar-Cuni, D. Ventura-Espinosa, S. V. Luis, E. García-Verdugo and J. A. Mata, A simple, safe and robust system for hydrogenation “without high-pressure gases” under batch and flow conditions using a liquid organic hydrogen carrier, *Green Chem.*, 2022, **24**(5), 2036–2043.
- 23 (a) C. R. Kennedy, D. Lehnerr, N. S. Rajapaksa, D. D. Ford, Y. Park and E. N. Jacobsen, Mechanism-Guided Development of a Highly Active Bis-thiourea Catalyst for Anion-Abstraction Catalysis, *J. Am. Chem. Soc.*, 2016, **138**(41), 13525–13528; (b) D. D. Ford, D. Lehnerr, C. R. Kennedy and E. N. Jacobsen, On- and Off-Cycle Catalyst Cooperativity in Anion-Binding Catalysis, *J. Am. Chem. Soc.*, 2016, **138**(25), 7860–7863; (c) D. D. Ford, D. Lehnerr, C. R. Kennedy and E. N. Jacobsen, Anion-Abstraction Catalysis: The Cooperative Mechanism of  $\alpha$ -Chloroether Activation by Dual Hydrogen-Bond Donors, *ACS Catal.*, 2016, **6**(7), 4616–4620.
- 24 J. L. Wen, X. R. Fan, R. C. Tan, H. C. Chien, Q. H. Zhou, L. W. Chung and X. M. Zhang, Brønsted-Acid-Promoted Rh-Catalyzed Asymmetric Hydrogenation of N-Unprotected Indoles: A Cocatalysis of Transition Metal and Anion Binding, *Org. Lett.*, 2018, **20**, 2143–2147.

